The Effects of Molecular Anions on the Chemistry of Dark Clouds

Catherine Walsh[1], Nanase Harada[2], Eric Herbst[3] and T. J. Millar[1]

cwalsh13@qub.ac.uk

ABSTRACT

We have investigated the role of molecular anion chemistry in pseudo-time-dependent chemical models of dark clouds. With oxygen-rich elemental abundances, the addition of anions results in a slight improvement in the overall agreement between model results and observations of molecular abundances in TMC-1 (CP). More importantly, with the inclusion of anions, we see an enhanced production efficiency of unsaturated carbon-chain neutral molecules, especially in the longer members of the families C_nH, C_nH_2, and HC_nN. The use of carbon-rich elemental abundances in models of TMC-1 (CP) with anion chemistry worsens the agreement with observations obtained in the absence of anions.

Subject headings: astrochemistry — ISM:abundances — ISM:clouds — ISM:molecules

1. INTRODUCTION

The possible existence of molecular anions (negatively charged ions) in the interstellar medium was discussed by Dalgarno & McCray (1973), Sarre (1980), and Herbst (1981). Herbst (1981) calculated that the large electron affinity of carbon-chain molecules and hydrocarbon radicals would lead to efficient radiative electron attachment rate coefficients for species with more than 4-5 atoms resulting in anion-to-neutral ratios on the order of a few percent. Confirmation of this hypothesis was achieved following the measurement of the rotational spectrum of the molecular anion, C_6H^-, in the laboratory by McCarthy et al. (2006). This measurement allowed the verification, from existing astronomical spectra (Kawaguchi et al. 1995), of the presence of C_6H^- in the envelope of the carbon rich evolved star, IRC+10216, at an abundance 1%-5% that of the neutral molecule. A successful astronomical search for C_6H^- in TMC-1(CP) by McCarthy et al. (2006) determined an anion-to-neutral ratio of $\sim 2.5\%$ in this source.

[1]Astrophysics Research Centre, School of Mathematics and Physics, Queen's University Belfast, University Road, Belfast, UK, BT7 1NN

[2]Department of Physics, The Ohio State University, Columbus, OH 43210

[3]Departments of Physics, Astronomy and Chemistry, The Ohio State University, Columbus, OH 43210

The rotational spectra of C_4H^-, C_8H^-, and C_3N^- have since been measured in the laboratory (Gupta et al. 2007; Thaddeus et al. 2008) with subsequent detections of C_4H^- (Cernicharo et al. 2007), C_8H^- (Remijan et al. 2007), and C_3N^- (Thaddeus et al. 2008) in the envelope of IRC+10216 and C_8H^- in TMC-1 (Brünken et al. 2007). Prompted by the observation of various carbon-chain molecules with large abundances in L1527, a class O/I protostar, by Sakai et al. (2008), C_6H^- was searched for and confirmed to be present in this source (Sakai et al. 2007) followed closely by the detection of C_4H^- (Agúndez et al. 2008). A survey of galactic molecular sources by Gupta et al. (2009) detected C_6H^- in two futher sources, the pre-stellar cloud, L1544, and the protostellar object, L1521F, suggestive of the ubiquitousness of molecular anions and C_6H^- in particular. Cernicharo et al. (2008) have attributed a series of rotational lines observed in the envelope of IRC+10216 to a new molecular anion, C_5N^-, although confirmation of this detection awaits successful measurement of the rotational spectrum of the molecule in the laboratory.

Following the identification of C_6H^- in the envelope of IRC+10216 and the detection in TMC-1, Millar et al. (2007) expanded the current release of the UMIST Database for Astrochemistry (Woodall et al. 2007) and the existing chemical network for the envelope of IRC+10216 (Millar et al. 2000) to include the molecular anions, C_n^- with n = 5 - 10 and C_nH^- with n = 4 - 10, using calculated rate coefficients for radiative electron attachment. Their results were limited to calculated anionic and precursor neutral column densities. For TMC-1 (CP), they found that the calculated 'early time' C_6H^- column density of 1.35×10^{11} cm^{-2} was very close to that measured by McCarthy et al. (2006), 1×10^{11} cm^{-2}. The calculated anion-to-neutral ratio of 5.2% was also in good agreement with the observed value of 2.5%. More recently, Harada & Herbst (2008) investigated the chemistry of the protostellar object, L1527, concentrating on the formation and depletion of molecular anions. Wakelam & Herbst (2008) considered the effects of negatively charged PAHs (polycyclic aromatic hydrocarbons) on dense cloud chemistry and found that PAH^- can replace electrons as the dominant negative charge carrier, an effect which depends strongly on the size of the PAHs considered.

The presence of molecular anions at significant abundances in the sources discussed above suggests that anions play a more significant role in the chemistry of astrophysical environments than previously believed. In this paper, we investigate the effects that the inclusion of molecular anion chemistry has on the chemistry of dark clouds by running simple pseudo-time-dependent models using the most recent release of the UMIST Database for Astrochemistry (Woodall et al. 2007), henceforth referred to as 'Rate06', and the latest OSU (Ohio State University) network, osu.03.2008 (see http://www.physics.ohio-state.edu/∼eric/). We compare our calculated fractional abundances for models both excluding and including anions with fractional abundances observed towards the cyanopolyyne (CP) peak of the dark cloud core, TMC-1, to determine the role that these species play in the gas-phase chemistry of dark clouds.

In Section 2, we describe our anionic chemistry and the initial chemical abundances and physical conditions adopted for our standard model. Section 3 contains detailed results obtained with and without anions for both networks, discusses the effects of anions on the chemistry of selected

classes of neutral species and compares our results with observations towards the molecular-rich region, TMC-1 (CP). Section 4 shows how our results are affected by the use of carbon-rich elemental abundances. Finally, in Section 5 we summarize our main findings.

2. CHEMICAL MODEL

We have expanded both Rate06 and the OSU network to include the molecular anions C_n^- (n = 3 - 10), C_nH^- (n = 4 - 10), and C_nN^- (n = 3, 5), building upon the previous work by Millar et al. (2007) by increasing the number of molecular anions studied and expanding the reaction set for each anion to incorporate new reaction channels and rate coefficients from recently published experimental work (Eichelberger et al. 2007). We use the dipole-enhanced version of Rate06, which includes an enhancement of ion-neutral rate coefficients at low temperatures for reactions where the neutral has a large, permanent dipole moment (> 0.9 Debye). The resulting rate coefficients have a $T^{-1/2}$ dependence at low temperatures (Herbst & Leung 1986; Woodall et al. 2007). A similar but not identical enhancement for the rate coefficients of ion-dipolar reactions is used in the OSU network (Herbst & Leung 1986).

The anions are formed primarily via radiative electron attachment,

$$X + e^- \rightarrow X^- + h\nu, \tag{1}$$

with updated attachment rate coefficients from recent theoretical calculations by Herbst & Osamura (2008). The hydrocarbon anions are destroyed through reactions with H, C, O, N, by photodetachment, and by mutual neutralization with abundant cations such as C^+. The destruction channels are listed in reactions (2) to (7) with m = 0 or 1:

$$\begin{aligned}
C_nH_m^- + H &\rightarrow C_nH_{m+1} + e^-, && (2)\\
C_nH_m^- + C &\rightarrow C_{n+1}H_m + e^-, && (3)\\
C_nH_m^- + O &\rightarrow CO + C_{n-1}H_m^-, && (4)\\
C_nH_m^- + N &\rightarrow CN + C_{n-1}H_m^-, && (5)\\
&\rightarrow CN^- + C_{n-1}H_m,\\
&\rightarrow C_3N^- + C_{n-3}H_m,\\
&\rightarrow C_5N^- + C_{n-5}H_m,\\
&\rightarrow H_mC_nN + e^-,\\
C_nH_m^- + h\nu &\rightarrow C_nH_m + e^-, && (6)\\
C_nH_m^- + X^+ &\rightarrow C_nH_m + X. && (7)
\end{aligned}$$

We have taken the rate coefficients for reaction (2) from Barkholtz et al. (2001) and for reactions (3), (4), and (5) from Eichelberger et al. (2007) for the species for which they were measured. In the absence of laboratory data, we have used estimated rate coefficients based on the experimental

measurements. The rate coefficients and reaction channels for reaction (5) are particularly uncertain because Eichelberger et al. (2007) were unable to detect associative detachment as a reaction channel, a potentially important synthetic route to the HC_nN molecules. We discuss the implications of these uncertainties in §3.2.5. The photo-detachment rate coefficients (reaction [6]) adopted are those listed in Table 1 of Millar et al. (2007), although in our model, this is an unimportant destruction mechanism as TMC-1 is well-shielded from external sources of UV radiation. The mutual neutralization reactions (reaction [7]) each have a rate coefficient $k = 7.5 \times 10^{-8}(T/300)^{-0.5}$ cm^3 s^{-1} as included by Harada & Herbst (2008) in their chemical model of L1527. We have assumed in all instances where appropriate that the products are obtained by a simple electron transfer. The C_3N^- chemistry we have added includes that listed in Table 1 of Harada & Herbst (2008) plus formation routes via the molecular anions, C_n^- and C_nH^- (eq. [5]), as observed in the experimental results of Eichelberger et al. (2007). We have included C_5N^- using the same destruction reactions and rate coefficients as for C_3N^- with a formation reaction rate coefficient (reaction [1]) calculated by E. Herbst (private communication) using the method of Herbst & Osamura (2008), to be $1.25 \times 10^{-7}(T/300)^{-0.5}$ cm^3 s^{-1}. Due to the inclusion of C_{10}^- and $C_{10}H^-$, we extrapolated both networks to include further hydrocarbon species containing 10 carbon atoms hence restricting the hydrocarbon chemistry to molecules with 11 carbon atoms or less.

We model the gas-phase chemistry of a dark cloud core by treating the source as an homogeneous, isotropic cloud with the constant physical parameters, $n(H_2) = 10^4$ cm^{-3}, T = 10 K, and $A_v = 10$ mag, using a cosmic-ray ionisation rate of 1.3×10^{-17} s^{-1}, and performing pseudo-time-dependent calculations, in which the chemistry evolves from initial abundances that are atomic except for molecular hydrogen, which is produced efficiently at an earlier stage. We employ the commonly used oxygen-rich low-metal elemental abundances, as listed in Table 1 and suggested originally by Graedel et al. (1982). Because pseudo-time-dependent gas-phase models of dark clouds are relatively predictive compared with more complex physical models, using such a simplified model helps us to accurately identify particular reactions or, more commonly, systems of reactions that are important and require further study.

Any comparison between our modelled results and observations in TMC-1 (CP) could, of course, be compromised by our use of a simplified model for a dark cloud. We would expect that employing a more detailed physical model could lead to different results from those presented here; however, such models are certainly not unique and therefore bring their own limitations. For example, recent work by Hassel et al. (2009, in preparation), in which a chemical dynamical-model following both the gas-phase and surface chemistry as a dense cloud forms via a shock, finds little difference in the gas-phase abundances of large molecules although the time-scales for formation are certainly different. Chemical factors, such as our neglect of accretion of gas-phase species onto dust grains, will also affect gas-phase abundances, although the timescales we are discussing here, $\sim 10^5$ yr, are only just at the stage where accretion becomes important for the conditions we have adopted.

3. RESULTS

Table 2 shows our calculated abundances using both networks for an assortment of molecules at the times of best agreement (typically $1 - 2 \times 10^5$ yr) for TMC-1 (CP) along with the observed values or upper limits. Model results are shown for calculations with and without anions. As can be seen, there is little difference between the results obtained with Rate06 and with the OSU network. We first discuss the anions and then consider families of neutral species strongly affected by the inclusion of anions. Throughout this section, we display the results from the models using Rate06 only because the results from the models using the OSU network are similar.

3.1. Anions

The calculated fractional abundances of the molecular anions, C_nH^- for n = 4, 6, 8, and 10, C_n^- for n = 4, 6, 8, and 10, and C_nN^- for n = 3 and 5, along with the neutral precursor or each anion, are plotted as a function of time in Figures 1 (a), 1 (b) and 1 (c), respectively. Because the main route of formation of the anions at all times is radiative electron attachment, the abundances of the anions follow that of their neutral precursors with both generally inversely proportional to molecular size. An exception is the abundance of C_4H^-, which at $\approx 10^5$ yr is comparable to that of C_6H^- because of the slow radiative electron attachment rate coefficient calculated for C_4H (Herbst & Osamura 2008). The larger abundance of C_5N^- compared with C_3N^- at all times, despite the smaller abundance of C_5N compared with C_3N, is due to the much larger electron attachment rate coefficient calculated for C_5N ($\sim 10^{-7}$ cm^3 s^{-1} compared with $\sim 10^{-10}$ cm^3 s^{-1}). Although the reaction rate coefficient for the formation of C_3N^- via dissociative attachment of HNC_3 is two orders of magnitude larger than that of the radiative electron attachment (see Table 1 of Harada & Herbst (2008)) the abundance of HNC_3 only reaches ~ 0.01 that of C_3N after $\sim 10^5$ yr when dissociative attachment becomes comparable with radiative attachment. The abundances of both the anions and neutrals peak around 10^5 yr and the destruction of the anions is dominated by reactions with H, C, O and C^+ (reactions [2], [3], [4], and [7], respectively).

In the absence of anions, the main destruction channels for C_nH are via reactions with C, O, and N:

$$C + C_nH \rightarrow C_{n+1} + H, \quad (8)$$

$$O + C_nH \rightarrow C_{n-1}H + CO, \quad (9)$$

$$N + C_nH \rightarrow C_{n-1}H + CN. \quad (10)$$

The inclusion of anions introduces radiative electron attachment (reaction [1]) as a destruction mechanism and it is this channel that dominates the destruction of the C_nH molecules at all times, excepting C_4H for which the destruction via the reaction with O is comparable.

Anionic chemistry also introduces new formation routes for the C_nH radicals. Ordinarily, these radicals are formed primarily via dissociative electron attachment to hydrocarbon cations as well

as via carbon insertion reactions (in reaction [11] m = 2 or 3):

$$\mathrm{C_nH_m}^+ + e^- \rightarrow \mathrm{C_nH} + \mathrm{H_{m-1}}, \quad (11)$$

$$\mathrm{C_{n+1}H}^+ + e^- \rightarrow \mathrm{C_nH} + \mathrm{C}, \quad (12)$$

$$\mathrm{C} + \mathrm{C_{n-1}H_2} \rightarrow \mathrm{C_nH} + \mathrm{H}. \quad (13)$$

New formation routes become important past $\sim 10^3$ yr when appreciable abundances of molecular anions have built up and C_nH is formed via associative electron detachment from carbon-chain anion and hydrocarbon anion precursors (see reactions [2] and [3]):

$$\mathrm{H} + \mathrm{C_n}^- \rightarrow \mathrm{C_nH} + e^-, \quad (14)$$

$$\mathrm{C} + \mathrm{C_{n-1}H}^- \rightarrow \mathrm{C_nH} + e^-. \quad (15)$$

Radiative electron attachment of the bare carbon-chain neutrals, C_n, as a destruction mechanism, only dominates prior to 10^4 yr, at which point reactions with O become comparable to this channel. As with the hydrocarbon radicals, the inclusion of bare carbon-chain anions opens up an additional formation route to the bare carbon-chain neutrals via associative electron detachment (reaction [3]):

$$\mathrm{C_{n-1}}^- + \mathrm{C} \rightarrow \mathrm{C_n} + e^-. \quad (16)$$

As can be seen in Table 2, the abundances for C_6H^- and C_8H^- are over-predicted at the time of best overall agreement by around an order of magnitude, with the abundance for C_4H^- around 50 times greater than the estimated upper limit by Thaddeus et al. (2008). There is a sharp decline in the predicted C_nH^- abundances at somewhat later times, however, as can be seen in Figure 1 (a). The abundance of C_4H^- only falls below the upper limit estimated by Thaddeus et al. (2008) after $\sim 10^6$ yr indicating that our electron attachment rate for C_4H is too large or that we are neglecting further destruction mechanisms for this species. In contrast to the anions already discussed, the predicted abundance of C_3N^- at the time of best overall agreement is in accordance with the upper limit determined by Thaddeus et al. (2008).

The calculated anion-to-neutral ratio, C_nH^-/C_nH for n = 4, 6, 8, and 10 is plotted as a function of time in Figure 2, along with the observed ratios for C_6H and C_8H. The calculated ratio for all species reaches a minimum around 10^5 yr, the same time that the peak in individual fractional abundances is reached. The model results for Rate06 yield 5.2% for the C_6H ratio and 3.9% for the C_8H ratio. These compare with the observed values for C_6H and C_8H of 1.6% and 4.6%, respectively.

3.2. Effects on Other Species

The main aim of this paper is to investigate the effects that the inclusion of anions has on the abundances and evolutionary behavior of other species in established chemical models. We have

identified several families of species that are affected; these include the neutral precursors of the anions, C_n, C_nH, and C_nN as well as the families of molecules C_nH_2 and HC_nN. The sensitivity of species in these families to the inclusion of anions can be seen in Table 2 for both networks.

3.2.1. C_n

Figure 3 (a) displays the fractional abundances of the neutral C_n molecules for n = 4, 6, 8, and 10 as a function of time for the models with and without anions. It is immediately apparent that the abundances of C_6, C_8, and C_{10} are enhanced at all times. The relative enhancement is more significant with increasing molecular size with little change in the abundance of C_4, in contrast to that of C_{10}, which increases by around 2 orders of magnitude in the presence of anions (see Table 2). As discussed previously in §3.1, introducing anions to the chemistry includes a new formation route via associative electron detachment (reaction [16]) whereby larger neutral carbon-chains can build up from smaller anionic precursors through repeated insertion of a carbon atom.

3.2.2. C_nH

Figure 3 (b) shows the fractional abundances of the C_nH molecules for the models with and without anions. As in Figure 3 (a) for C_n, there is an obvious enhancement of the larger hydrocarbon radicals, C_6H, C_8H, and $C_{10}H$, at all times prior to 10^6 yr with the enhancement increasing with molecular size. The addition of anions introduces two new formation mechanisms via associative detachment from bare carbon-chain anions (reaction [14]) and hydrocarbon anions (reaction [15]), again introducing a new route to the formation of larger hydrocarbon radicals from smaller ones. At the time of overall best agreement, as seen in Table 2, the inclusion of anions enhances the abundance of C_6H from a value which is ≈ 3 times smaller than observed to one ≈ 3 times larger than observed, while the abundance of C_8H is enhanced from a value ≈ 4 times smaller to one $\approx$ 14 times larger than observed. There is no enhancement of the C_4H abundance, which remains a factor of ≈ 5 below the observed value. As in the case for the hydrocarbon anions, the abundances of both C_6H and C_8H reach their best agreement with observation at slightly later times, while that of C_4H diminishes further.

3.2.3. C_nN

The fractional abundances of the C_nN radicals, with n = 3, 5, 7, and 9, are plotted in Figure 3 (c), as a function of time. The abundances of all of these species are enhanced in the model with anions, compared with the results for the model without anions, prior to $\sim 3 \times 10^5$ yr. As with the carbon chains and hydrocarbons, the biggest relative enhancement is seen in the larger species, C_7N and C_9N, with the peak fractional abundance of C_9N increasing by around 2 orders of

magnitude from $\sim 10^{-13}$ to $\sim 10^{-11}$. When anions are not included in the model, the main routes to the formation of C_nN for n = 5, 7, and 9 are

$$H_2C_nN^+ + e^- \rightarrow C_nN + H_2, \quad (17)$$
$$H_3C_nN^+ + e^- \rightarrow C_nN + H_2 + H, \quad (18)$$
$$N + C_nH \rightarrow C_nN + H, \quad (19)$$

with destruction via reactions with O and N atoms. Reaction (17) dominates the formation up to $\sim 10^5$ yr after which reaction (19) is comparable to or dominates over reaction (17). For C_3N, reaction (19) is the main route of formation at all times.

The inclusion of anions introduces a new formation route via the bare carbon chain anions, C_n^-:

$$N + C_n^- \rightarrow C_nN + e^-, \quad (20)$$

and it is this route that dominates the formation for n = 5, 7, and 9 up to $\sim 10^5$ yr after which reactions (17) and (19) take over. As in the case without anions, the main formation route for C_3N is through reaction (19). As the abundances of the C_nH radicals are enhanced with the inclusion of anions this also increases the influence of reaction (19) over that of reaction (17) in contrast to the case without anions.

3.2.4. C_nH_2

Whilst the effect on the abundances of C_n and C_nH due to the inclusion of their respective anions may come as little surprise, other families of species are also affected. Figure 4 (a) shows the time-dependent fractional abundance of C_nH_2 for n = 4, 6, 8, and 10. The abundances of all species are enhanced at all times in the model with anions included, with a more marked effect for C_8H_2 and $C_{10}H_2$. In the absence of anions, the C_nH_2 species form via dissociative recombination, e.g. reactions (21) and (22), or via neutral-neutral reactions,

$$C_nH_3^+ + e^- \rightarrow C_nH_2 + H, \quad (21)$$
$$C_nH_4^+ + e^- \rightarrow C_nH_2 + H_2, \quad (22)$$
$$C_{n-2}H_2 + C_2H \rightarrow C_nH_2 + H. \quad (23)$$

Adding anions to the chemistry opens a new synthetic channel via associative detachment of the hydrocarbon anions, C_nH^-, with H atoms (reaction [2]) and it is this channel which dominates up to $\sim 10^6$ yr. The C_nH_2 species in the dominant polyyne isomer, HC_nH, are not observable via rotational spectroscopy because this isomer has zero dipole moment. The cumulene carbene forms H_2C_n are detectable but in general cannot be formed by associative detachment because the reactions are endothermic (Herbst & Osamura 2008).

3.2.5. HC_nN

Figure 4 (b) shows the abundances of the HC_nN molecules for n = 3, 5, 7, and 9 and again we see a marked enhancement in the abundances of all species when anions are included in the networks. The synthesis of the larger cyanopolyyne molecules proceeds (as for many neutral molecules) via the dissociative recombination of a cationic molecular precursor:

$$H_2C_nN^+ + e^- \rightarrow HC_nN + H, \quad (24)$$

$$H_3C_nN^+ + e^- \rightarrow HC_nN + 2H, \quad (25)$$

with a secondary route through the reaction

$$C_{n-1}H_2 + CN \rightarrow HC_nN + H. \quad (26)$$

The addition of anions to the chemistry enhances the abundances of the C_nH_2 species which increases the effect of reaction (26). There is also a more subtle influence on the abundances of $H_2C_nN^+$ and $H_3C_nN^+$ which are produced via a series of different reaction pathways originating from hydrocarbon cations, $C_nH_m{}^+$, the abundances of which are enhanced in the presence of molecular anions. Examples of this type of reaction are

$$C_4H_2{}^+ + HC_{n-4}N \rightarrow H_3C_nN^+ + h\nu, \quad (27)$$

$$C_2H_2{}^+ + HC_{n-2}N \rightarrow H_3C_nN^+ + h\nu. \quad (28)$$

In addition, the inclusion of C_3N^- and C_5N^- introduces new formation mechanisms for HC_3N and HC_5N via associative electron detachment of each anion with H atoms. This reaction has a fast rate coefficient, on the order of 10^{-9} cm^3 s^{-1}, which has a large effect on the abundance of HC_5N, in particular.

The destruction of the hydrocarbon anions C_nH^- via reactions with atomic N (reaction [5]) has an associative detachment channel, which leads to the cyanopolyyne molecules for n = 3, 5, 7, and 9. The rate coefficients for these reactions have been derived from experimental data by Eichelberger et al. (2007) who found that the reactions of anions with an even number of carbon atoms proceed slowly, with rate coefficients on the order of 10^{-11} cm^3 s^{-1}. Branching ratios for the products were not determined, although contact with the authors led to their agreement that the associative detachment channel to form the cyanopolyynes could have a branching fraction of ≈ 0.5. For reactions with odd numbers of carbons in the hydrocarbon anions, i.e. n = 3, 5, 7, and 9, we have assumed that the reactions proceed with a rate coefficient the same order of magnitude, with an associative detachment channel that has a branching fraction 50% of the total rate. Inclusion of this reaction channel has little effect on the HC_nN abundances due to the small rate coefficient used; however, we have also run a model with this reaction channel proceeding using a larger rate coefficient of 10^{-10} cm^3 s^{-1}, on the basis that the reactions between C_nH^- species with odd values of n and atomic nitrogen are spin allowed. The results from this "third" model are also shown in Figure 4 (b) (dotted lines) in addition to the results from the model without anions

(solid lines) and our standard model with anions (dotted-dashed lines). The associative detachment channel futher enhances the abundances of HC_7N and HC_9N in particular, two molecules for which existing chemical networks have difficulty reproducing the observed abundances. At the time of best agreement in the third model (1.6×10^5 yr), the abundances are in vastly better agreement with the observed abundances listed in Table 2 although they still lie somewhat below observational values.

3.3. Comparison of Model Results with Observed Abundances in TMC-1 (CP)

In Table 2, the abundances of species that agree to within one order of magnitude at the time of best overall agreement are in normal type, those predicted to be more than one order of magnitude too large are in bold italic type and those predicted to be more than one order of magnitude too small are in Roman bold type. It is immediately apparent that the inclusion of anions in both networks does not have a dramatic effect on the agreement with observation. Specifically, removing the anions from Rate06 reduces the percentage of molecular abundances that lie within one order of magnitude of those observed from $\sim 66\%$ (35 out of 53 species) to $\sim 63\%$ (32 out of 51 species). The improvement when anions are included is minor but noticeable.

Important molecules for which the inclusion of anions improves agreement with observation are HC_5N, HC_7N and HC_9N (as discussed in detail in §3.2.5), while the only molecule for which the inclusion of anions has a significantly detrimental effect on agreement with observation is C_8H. Both networks have difficulty reproducing the observed abundances of the sulfur-containing molecules, H_2S, SO, C_2S, SO_2, and HCS^+, due in part to the choice of the low initial elemental abundance for S^+. A slightly higher choice can improve agreement strongly (Smith et al. 2004). With our current elemental abundance, SO, C_2S, and SO_2, all reach good agreement with observation at later times between 3×10^5 and 6×10^5 yr. Later times than the time of best agreement may pertain to cloudlets in TMC-1 other than the CP region, where most complex species peak (Park et al. 2006). The calculated abundances of several organic molecules are much lower than that observed, especially for CH_3OH, CH_3CCH, and CH_2CHCN. All these species are difficult to synthesize using gas-phase processes only. It has been thought for some time that saturated species, in particular, CH_3OH, form on the surfaces of dust grains through the repeated hydrogenation of CO (Tielens & Hagen 1982), a claim backed up by some experimental evidence (Watanabe et al. 2004).

The relatively small differences observed when anions are included in our models are partially due to their low abundance compared with electrons, as shown in Figure 5 for Rate06. This is in contrast to the findings of Wakelam & Herbst (2008) who compute that after $\sim 10^2$ yr, negatively charged small PAHs are the dominant negative charge carrier with an abundance almost two orders of magnitude larger than the electron abundance at steady state. This effect diminishes with increasing PAH size (and thus decreasing fractional abundance). With PAHs the dominant negative charge carriers, the overall ionization decreases because atomic positive ions are more readily neutralized by PAH^- than by bare electrons. This decrease results in increases in the

abundances of positively charged molecular ions, which in turn lead to increases in the abundances of unsaturated neutral species such as the cyanopolyynes and saturated species such as methanol. Despite the increase in the abundance of methanol, however, the computed abundance lies well below the observed one. Future models should investigate the effects of adding both negatively charged PAHs as well as molecular anions.

4. VARIATIONS IN INITIAL ABUNDANCES

In this work we have used oxygen-rich initial abundances with a carbon-to-oxygen ratio of ~ 0.4. Previous modellers (Terzieva & Herbst 1998; Roberts & Herbst 2002; Smith et al. 2004; Wakelam et al. 2006) have found that to get better agreement with observations of chemical abundances in TMC-1 (CP), a higher ratio is required, usually $\gtrsim 1$. The most successful of the models listed is the work of Wakelam et al. (2006) who report that with a carbon-to-oxygen ratio of 1.2, 86% of the abundances can be fit if the observations are given an uncertainty of a factor of five. These authors use as a criterion for success an overlap between Gaussian distributions of modeling and observational results for each species, the former obtained by a Monte Carlo analysis from uncertainties in both reaction rate coefficients and physical conditions.

To test the effects that the addition of anions has on carbon-rich models of the chemistry of dark clouds, we have run models using both networks with a carbon-to-oxygen ratio of 1.2, with and without anions. Using Rate06 without anions, at the time of best agreement, 40 out of 51 species agree with observation to within one order of magnitude, an improvement similar to that found by Wakelam et al. (2006). In contrast to the oxygen-rich initial conditions, we find that the addition of anions in the carbon-rich case worsens our agreement with observation for both networks. For Rate06 with anions, the agreement is reduced to 37 out of 53 species at the optimum time. The results with the OSU network are similar. In the carbon-rich case, the increased synthetic power obtained upon adding anions is magnified due to the increased carbon budget so that the calculated abundances of long-chain carbon molecules substantially overshoot the observed abundances, thus worsening the overall agreement with observation. Even in the case without anions, the better agreement obtained with carbon-rich abundances may be at least partially due to an edge effect, in which much of the carbon budget ends up in the longer-chained species. Since many of these species have not been observed in TMC-1, it is difficult to say whether the enhanced agreement is real or a result of the chemistry being limited to molecules with 11 carbon atoms or fewer.

5. SUMMARY

We have modelled the gas-phase chemistry of a dark cloud to investigate the role of molecular anions in the overall chemistry. We have used the simple pseudo-time-dependent gas-phase model, which can be criticized both for its lack of dynamics during the chemical evolution and for the

lack of processes involving dust grains. Nevertheless, our use of the simplified gas-phase model has enabled us to highlight the direct chemical effects of the addition of molecular anions on our existing standard networks.

The inclusion of anions has only a slight positive effect on the success of both the Rate06 and OSU networks in reproducing the observed abundances in TMC-1 (CP) with the pseudo-time-dependent model. The most significant effect of the addition of anionic species is the enhancement in the abundances of several families of carbon-chain molecules, namely, C_n, C_nH, C_nH_2, C_nN, and HC_nN, by providing new formation routes to the larger members of each family via smaller molecules. We get much better agreement with abundances observed in TMC-1 (CP) for the cyanopolyyne molecules, in particular, and would urge further experimental measurements of the rate coefficient and product channels for reaction (5), which we have shown to be an important formation route to the HC_nN molecules. This 'catalytic' effect could be at least partially artificial because our chemistry is capped at molecules with 11 or fewer carbon atoms, so that we may be witnessing an 'edge' effect whereby molecules move up the chain through repeated addition of a carbon atom with the larger molecules becoming a 'sink' for carbon. To check if this is the case, it may be necessary to add larger carbon-chain species to the chemistry, similar to that done by Millar et al. (2000) for their chemical model of the shell of IRC+10216. Credence is given to our results, however, as the peak abundances of the molecules remain inversely proportional to molecular size even given this catalytic effect.

We have also investigated the effect of using carbon-rich elemental abundances. Running models using both networks, with and without anions, with a carbon-to-oxygen ratio of 1.2, we find that we get improved agreement for TMC-1 (CP) over the oxygen-rich case for the carbon-rich models without anions. The inclusion of anions, however, worsens our agreement with observation due to the excessively enhanced synthesis of long-chain carbon species.

Many of the large number of reactions involving anions that have been added to the reaction sets remain poorly understood. Although our results here show that the inclusion of anions does not have a dramatic effect on the chemistry, these conclusions must remain tentative pending further experimental work to determine more accurate rate coefficients. It is anticipated that in the near future, further anionic species will be discovered as laboratory measurements of the rotational spectra of candidate molecules increase in number, and we would expect that existing chemical networks will be expanded to incorporate molecular anions as standard. The current (anionic and non-anionic) releases of both Rate06 and the OSU network are available online at http://www.udfa.net/ and http://www.physics.ohio-state.edu/∼eric/, respectively.

We would like to thank Valentine Wakelam and Martin Cordiner for their input and advice. Astrophysics at Queen's University Belfast is supported by a grant from the Science and Technology Facilities Council. C. W. is supported by scholarship from the Northern Ireland Department of Employment and Learning. E. H. acknowledges the support of the National Science Foundation for his research program in astrochemistry.

REFERENCES

Agúndez, M., Cernicharo, J., Guélin, M., Gerin, M., McCarthy, M. C. & Thaddeus, P. 2008, A&A, 478, L19

Barkholtz, C., Snow, T. P. & Bierbaum, V. M. 2001, ApJ, 547, L171

Brünken, S., Gupta, H., Gottlieb, C. A., McCarthy, M. C. & Thaddeus, P. 2007, ApJ, 664, L43

Cernicharo, J., Guélin, M., Agúndez, M., Kawaguchi, K., McCarthy, M. & Thaddeus, P. 2007, A&A, 467, L37

Cernicharo, J., Guélin, M., Agúndez, M., McCarthy, M. & Thaddeus, P. 2008, ApJ, 688, L83

Dalgarno, A., & McCray, R. A. 1973, ApJ, 181, 95

Eichelberger, B., Snow, T. P., Barckholtz, C. & Bierbaum, V. B. 2007, ApJ, 667, 1283

Graedel, T. E., Langer, W. D. & Frerking, M. A. 1982, ApJS, 48, 321

Gupta, H., Brünken, S., Tamassia, F., Gottleib, C. A., McCarthy, M. C. & Thaddeus, P. 2007, ApJ, 655, L57

Gupta, H., Gottlieb, C. A., McCarthy, M. C. & Thaddeus P. 2009, ApJ, 691, 1494

Harada, N. & Herbst, E. 2008, ApJ, 685, 272

Hassel, G. E., Herbst, E. & Bergin, E. A. 2009, in preparation

Herbst, E. 1981, Nature, 289, 656

Herbst, E. & Leung, C. M. 1986, ApJ, 310, 378

Herbst, E. & Osamura, Y. 2008 ApJ, 679, 1670

Kawaguchi, K., Kasai, Y., Ishikawa, S. & Kaifu, N, 1995, PASJ, 47, 853

McCarthy, M. C., Gottlieb, C. A., Gupta, H. & Thaddeus, P. 2006, ApJ, 652, L141

Millar, T. J., Herbst, E. & Bettens, R. P. A. 2000, MNRAS, 316, 195

Millar, T. J., Walsh, C., Cordiner, M. A., Ní Chuimín, R. & Herbst, E. 2007, ApJ, 662, L87

Park, I. H., Wakelam, V., & Herbst, E. 2006, A&A, 449,, 631

Remijan, A. J., Hollis, J. M., Cordiner, M. A., Millar, T. J., Markwick-Kemper, A. J. & Jewell, P. R. 2007, ApJ, 664, L47

Roberts, H. & Herbst, E. 2002, A&A, 395, 233

Sakai, N., Sakai, T., Osamura, Y. & Yamamoto, S. 2007, ApJ, 667, L65

Sakai, N., Sakai, T., Hirota, T. & Yamamoto, S. 2008, ApJ, 672, 371

Sarre, P. J. 1980, JCPPC, 77, 769

Smith, I. W. M., Herbst, E. & Chang, Q. 2004, MNRAS, 350, 323

Terzieva, R. & Herbst, E. 1998, ApJ, 501, 207

Thaddeus, P., Gottlieb, C. A., Gupta, H., Brünken, S. & McCarthy, M. C. 2008, ApJ, 677, 1132

Tielens, A. G. G. M. & Hagen, W. 1982, A&A, 114, 245

Wakelam, V., Herbst, E. & Selsis, F. 2006, A&A, 451, 551

Wakelam, V. & Herbst, E. 2008, ApJ, 680, 371

Watanabe, N., Nagaoka, A., Shiraki, T. & Kouchi, A. 2004, ApJ, 616, 638

Woodall, J., Agúndez, M., Markwick-Kemper, A. J. & Millar, T. J. 2007, A&A, 466, 1197

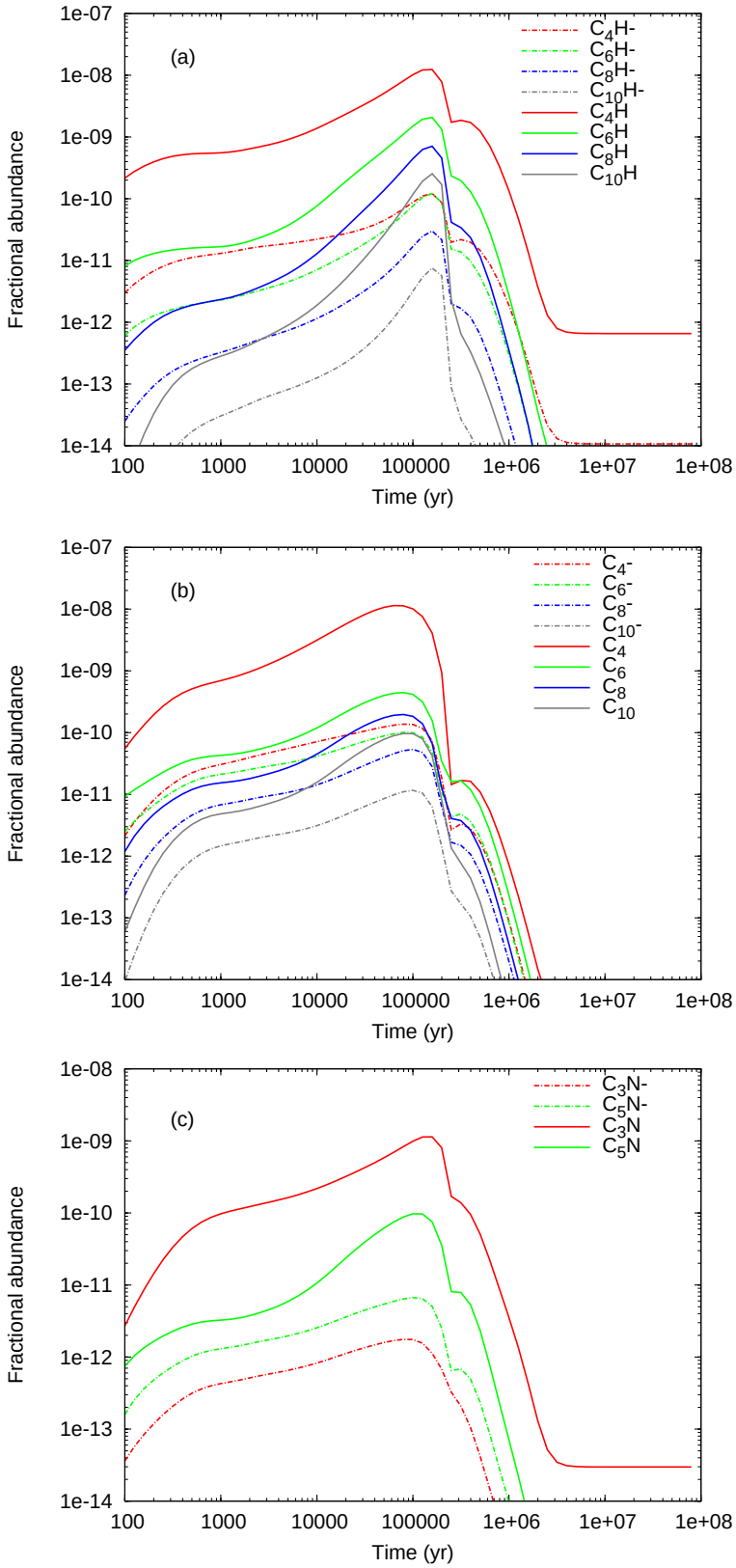

Fig. 1.— The abundances with respect to H_2 density of (a) C_nH^- for n = 4, 6, 8, and 10, (b) C_n^- for n = 4, 6, 8, 10, and (c) C_nN^- for n = 3, 5 and their corresponding neutral analogs, as a function of time.

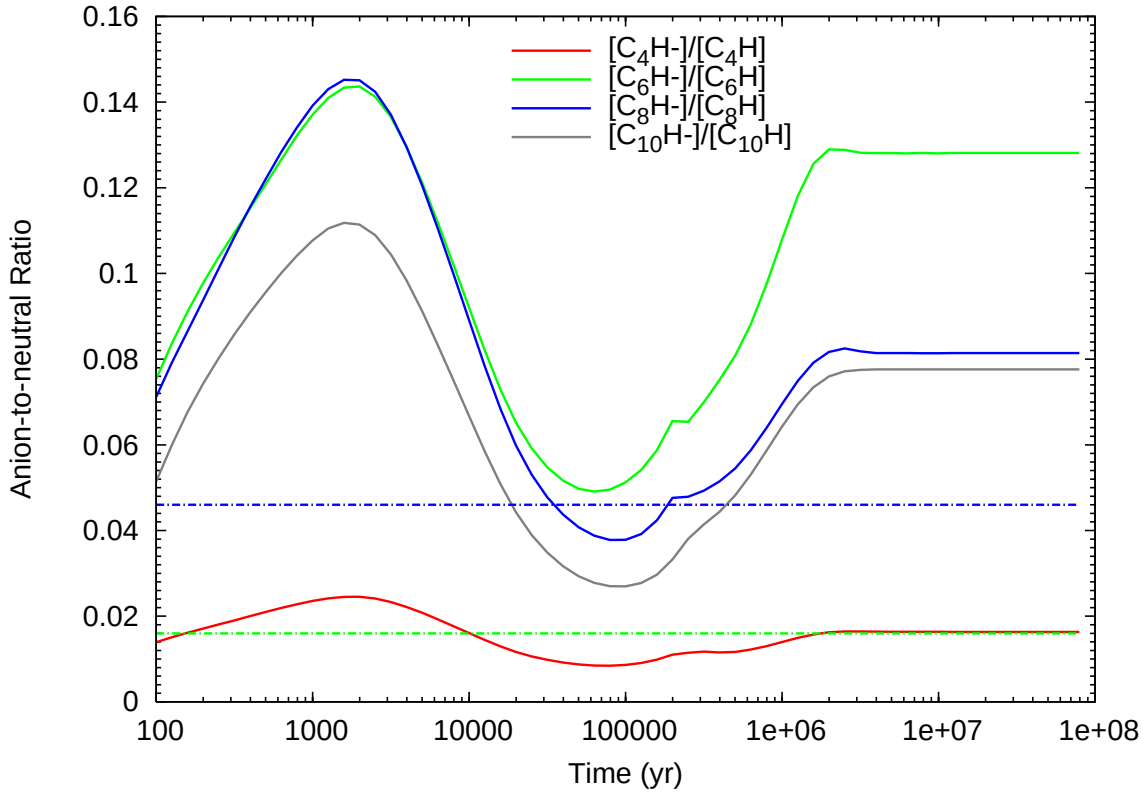

Fig. 2.— The anion-to-neutral ratio C_nH^-/C_nH for n = 4, 6, 8, and 10, as a function of time. The dotted-dashed horizontal lines are the observed ratios for C_6H^- and C_8H^-.

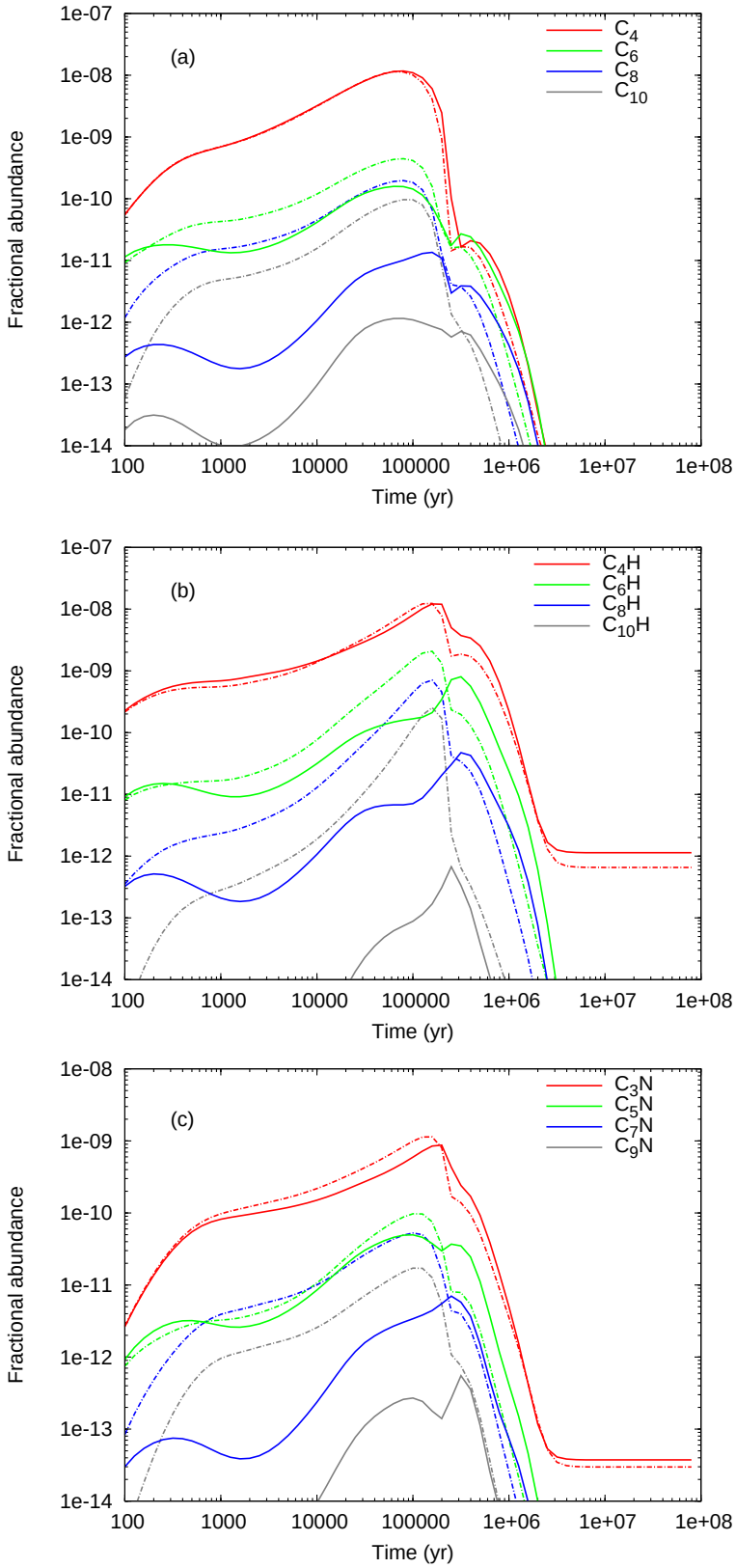

Fig. 3.— The abundances with respect to H_2 density of (a) C_n for n = 4, 6, 8, and 10, (b) C_nH for n = 4, 6, 8, and 10, and (c) C_nN for n = 3, 5, 7, and 9, as a function of time, with (dotted-dashed lines) and without (solid lines) anions.

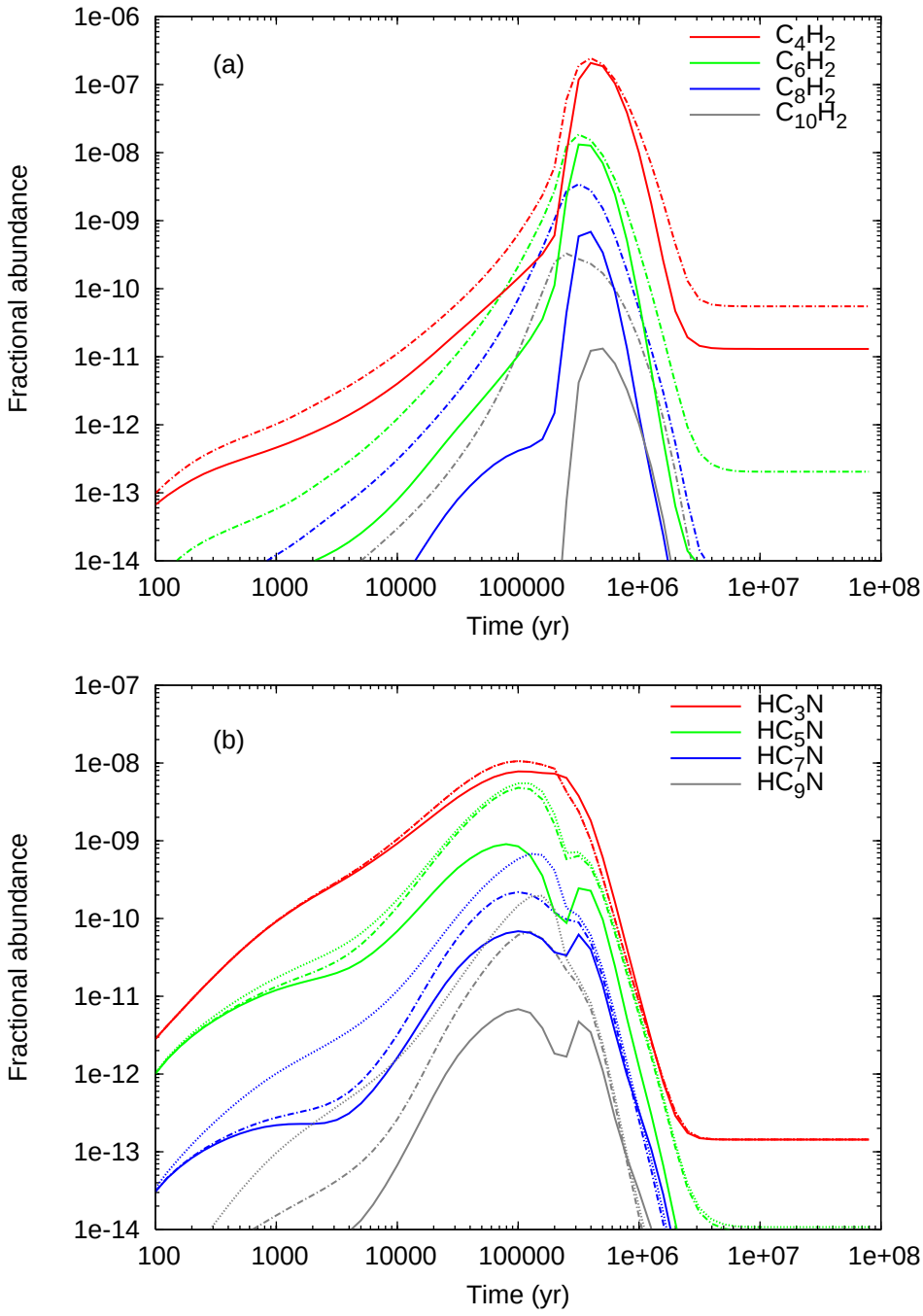

Fig. 4.— The abundances with respect to H_2 density of (a) C_nH_2 for n = 4, 6, 8, and 10, and (b) HC_nN for n = 3, 5, 7, and 9, as a function of time, with (dotted-dashed lines) and without (solid lines) anions. The dotted lines in the HC_nN plot are results from the model using the larger rate coefficients for $C_nH^- + N \rightarrow HC_nN + e^-$.

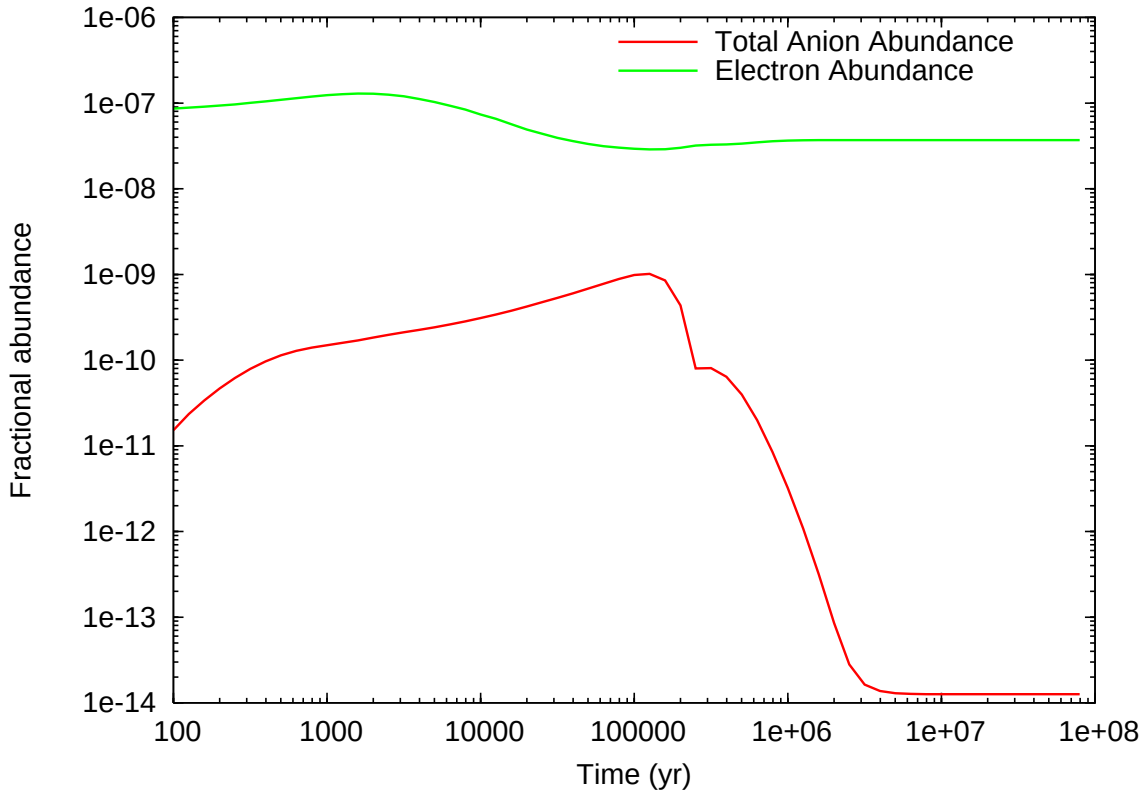

Fig. 5.— The electron and total anionic abundances with respect to H_2 as functions of time computed with Rate06.

Table 1. Initial Species and Elemental Abundances With Respect to Hydrogen Nuclear Density

Element	Initial Fractional Abundance
H_2	5.00×10^{-1}
He	1.40×10^{-1}
C	7.30×10^{-5}
N	2.14×10^{-5}
O	1.76×10^{-4}
S^+	2.00×10^{-8}
Si^+	3.00×10^{-9}
Na^+	3.00×10^{-9}
Mg^+	3.00×10^{-9}
Fe^+	3.00×10^{-9}
P^+	3.00×10^{-9}
F	2.00×10^{-8}
Cl	3.00×10^{-9}

References. — Graedel et al. (1982)

Table 2. Calculated Abundances of Families of Species With Respect to H_2 and Comparison with Observed Species in TMC-1 (CP)

Species	Observed[a]	Rate06 Without Anions	Rate06 With Anions	OSU Without Anions	OSU With Anions
			Anions		
C_4H^-	$< 2.3(-12)^b$	...	1.1(-10)	...	1.1(-10)
C_6H^-	$1.2(-11)^c$	...	1.0(-10)	...	1.1(-10)
C_8H^-	$2.1(-12)^c$	...	2.5(-11)	...	2.5(-11)
C_3N^-	$< 7.0(-11)^b$	...	1.6(-12)	...	3.6(-12)
			C_n		
C_4	...	6.1(-09)	3.8(-09)	1.8(-08)	1.6(-08)
C_6	...	6.7(-11)	3.2(-10)	1.1(-10)	4.7(-10)
C_8	...	1.4(-11)	1.4(-10)	2.7(-11)	2.0(-10)
C_{10}	...	8.6(-13)	7.9(-11)	4.3(-12)	9.2(-11)
			C_nH		
C_4H	$6.1(-08)^c$	1.2(-08)	1.2(-08)	6.5(-09)	9.8(-09)
C_6H	$7.5(-10)^c$	2.1(-10)	1.9(-09)	1.8(-10)	2.1(-09)
C_8H	$4.6(-11)^c$	1.3(-11)	***6.3(-10)***	1.3(-11)	***6.3(-10)***
$C_{10}H$	...	1.7(-13)	1.9(-10)	1.5(-12)	1.8(-10)
			C_nH_2		
C_4H_2	...	3.2(-10)	1.2(-09)	1.4(-10)	1.1(-09)
C_6H_2	...	3.6(-11)	4.6(-10)	3.6(-11)	5.9(-10)
C_8H_2	...	6.1(-13)	1.6(-10)	6.9(-13)	2.0(-10)
$C_{10}H_2$	...	4.3(-17)	3.2(-11)	3.6(-17)	3.5(-11)

Table 2—Continued

Species	Observed[a]	Rate06 Without Anions	Rate06 With Anions	OSU Without Anions	OSU With Anions
			C_nN		
C_3N	6.0(-10)[b]	8.5(-10)	1.1(-09)	6.0(-10)	1.0(-09)
C_5N	...	3.8(-11)	9.7(-11)	3.3(-11)	1.5(-10)
C_7N	...	4.4(-12)	5.0(-11)	4.4(-12)	6.2(-11)
C_9N	...	1.8(-13)	1.7(-11)	2.9(-13)	2.0(-11)
			HC_nN		
HNC_3	6.0(-11)	2.8(-11)	2.4(-11)	1.2(-10)	1.5(-10)
HC_5N	4.0(-09)	**3.6(-10)**	4.6(-09)	**2.2(-10)**	3.1(-09)
HC_7N	1.1(-09)	**5.4(-11)**	2.1(-10)	**1.6(-11)**	1.2(-10)
HC_9N	4.5(-10)	**3.9(-12)**	6.8(-11)	**1.9(-12)**	**3.6(-11)**
			Remaining Species Observed in TMC-1		
CH	2.0(-08)	5.5(-09)	6.2(-09)	6.6(-09)	7.4(-09)
NH_3	2.0(-08)	1.5(-08)	1.3(-08)	1.4(-08)	1.3(-08)
OH	2.0(-07)	4.0(-08)	3.8(-08)	2.7(-08)	2.7(-08)
H_2O	$\leqslant$7.0(-08)	***1.2(-06)***	***1.4(-06)***	***1.2(-06)***	***1.4(-06)***
C_2	5.0(-08)	**2.3(-09)**	**2.9(-09)**	**3.7(-09)**	**3.8(-09)**
C_2H	2.0(-08)	1.4(-08)	1.6(-08)	1.1(-08)	1.6(-08)
CN	5.0(-09)	2.6(-08)	2.8(-08)	8.3(-09)	9.9(-09)
HNC	2.0(-08)	2.4(-08)	3.3(-08)	2.0(-08)	2.6(-08)
HCN	2.0(-08)	3.4(-08)	4.8(-08)	1.9(-08)	2.5(-08)
$HCNH^+$	2.0(-09)	**1.9(-10)**	4.5(-10)	2.4(-10)	4.7(-10)
CO	8.0(-05)	1.0(-04)	9.4(-05)	9.6(-05)	9.8(-05)
N_2H^+	4.0(-10)	1.1(-10)	1.1(-10)	1.9(-10)	1.7(-10)
HCO^+	8.0(-09)	4.0(-09)	4.7(-09)	4.0(-09)	5.0(-09)
NO	3.0(-08)	3.4(-08)	2.4(-08)	9.1(-09)	8.9(-09)
H_2CO	5.0(-08)	**1.1(-09)**	**1.3(-09)**	8.6(-08)	8.2(-08)

Table 2—Continued

Species	Observed[a]	Rate06		OSU	
		Without Anions	With Anions	Without Anions	With Anions
CH_3OH	3.0(-09)	**5.1(-13)**	**4.9(-13)**	**1.2(-13)**	**1.6(-13)**
O_2	⩽7.7(-08)	1.1(-07)	7.5(-08)	7.3(-08)	6.9(-08)
H_2S	5.0(-10)	**7.2(-12)**	**6.9(-12)**	**9.2(-12)**	**9.1(-12)**
C_3H	1.0(-08)	1.4(-08)	1.7(-08)	1.0(-08)	1.7(-08)
C_3H_2	1.1(-08)	2.3(-08)	1.5(-08)	1.2(-08)	1.1(-08)
CH_2CN	5.0(-09)	**2.4(-10)**	**4.0(-10)**	**2.2(-10)**	**3.3(-10)**
C_2O	6.0(-11)	4.3(-11)	7.5(-11)	1.5(-11)	1.9(-11)
CH_3CCH	6.0(-09)	**4.1(-12)**	**4.2(-12)**	**4.0(-12)**	**4.6(-12)**
CH_3CN	6.0(-10)	9.3(-10)	1.9(-09)	4.9(-10)	7.9(-10)
H_2CCO	6.0(-10)	***7.1(-09)***	***9.4(-09)***	***2.1(-08)***	***2.3(-08)***
CS	4.0(-09)	4.9(-09)	3.9(-09)	7.1(-10)	6.2(-10)
CH_3CHO	6.0(-10)	**4.2(-11)**	**4.4(-11)**	**1.1(-12)**	**1.3(-12)**
HCS^+	4.0(-10)	**2.1(-12)**	**2.9(-12)**	**8.2(-13)**	**9.8(-13)**
H_2CS	7.0(-10)	1.8(-09)	1.6(-09)	2.4(-10)	2.1(-10)
HCOOH	2.0(-10)	2.0(-09)	***2.4(-09)***	7.5(-10)	1.0(-09)
SO	2.0(-09)	**5.4(-11)**	**3.8(-11)**	**6.6(-11)**	**5.7(-11)**
HC_2NC	5.0(-10)	...	...	2.2(-10)	3.8(-10)
HNC_3	6.0(-11)	2.8(-11)	2.4(-11)	1.2(-10)	1.5(-10)
HC_3NH^+	1.0(-10)	1.1(-11)	2.3(-11)	5.1(-11)	1.3(-10)
C_3O	1.0(-10)	6.0(-10)	7.5(-10)	***1.5(-09)***	***2.1(-09)***
CH_2CHCN	4.0(-09)	**5.8(-13)**	**1.3(-12)**	**1.2(-13)**	**2.0(-13)**
C_2S	8.0(-09)	**7.9(-10)**	**7.6(-10)**	**4.2(-10)**	**5.0(-10)**
OCS	2.0(-09)	4.8(-10)	4.6(-10)	**1.1(-10)**	**1.2(-10)**
SO_2	1.0(-09)	**5.4(-13)**	**2.8(-13)**	**8.2(-13)**	**6.7(-13)**
CH_3C_4H	4.0(-10)	**2.3(-11)**	**3.4(-11)**	**3.8(-11)**	6.3(-11)
CH_3C_3N	8.0(-11)	3.0(-10)	4.7(-10)	9.8(-12)	2.2(-11)
C_3S	1.0(-09)	4.2(-10)	4.0(-10)	1.3(-10)	1.6(-10)
Agreement	...	32/51	35/53	33/52	36/54

[a]As collated by Smith et al. (2004) unless otherwise stated

[b]Thaddeus et al. (2008)

[c]Brünken et al. (2007)

Note. — a(b) represents a $\times$ 10^{b}

Note. — Calculated abundances refer to the time of best agreement for each model, which is 1-2 $\times 10^{5}$ yr

Note. — Normal type refers to modelled abundances which agree with observation to within one order of magnitude, bold type refers to those more than an order of magnitude smaller, and bold italic type refers to those which are more than one order of magnitude larger.